A preliminary computational investigation of a macro-model for vuggy porous media*

T. Arbogast[ab], D. S. Brunson[ab], S. L. Bryant[ac], and J. W. Jennings, Jr.[d].

[a]Center for Subsurface Modeling, Institute for Computational Engineering and Sciences, 1 University Station C0200, Austin, Texas 78712

[b]Department of Mathematics, The University of Texas at Austin, 1 University Station C1200, Austin, Texas 78712

[c]Department of Petroleum and Geosystems Engineering, The University of Texas at Austin, 1 University Station C0300, Austin, Texas 78712

[d]Bureau of Economic Geology, The University of Texas at Austin, 1 University Station E0630, Austin, Texas 78712

A *vug* is a relatively large void region or cavity in a rock. A vuggy porous medium has many vugs scattered throughout its extent; moreover, these vugs may be interconnected. A Darcy-Stokes system of equations is needed to describe the flow on the micro-scale. Recently a macro-model of flow was derived by mathematical homogenization that provides the effective permeability of a vuggy medium. In this paper we present two computational studies to illustrate and verify this macro-model. In the first study, we illuminate the nature of the effective permeability itself by considering vuggy media with (i) layered vugs, (ii) meandering vug channels, (iii) constricted vug channels, and (iv) disconnected vugs. We find that vug connectivity is the most critical variable in predicting macroscopic properties. In the second study, we consider the macro-model. We compare fluid flow in a vuggy medium on the micro-scale to that on the macro-scale. We find support for the macro-model, and again find that vug interconnectivity is the critical variable to preserve in the upscaling process.

1. INTRODUCTION

The geometry and distribution of natural fractures govern the flow of groundwater in most carbonate aquifers. However, some contain relatively large *vugs* (voids or cavities that are much larger than inter-granular pores) that are not part of a fracture system. Vugular fabrics in carbonate rocks generally fall into two groups. The first is composed of non-tectonic fractures, karst conduits, caverns and collapse breccia, and it is normally associated with karsting and massive dissolution. The second group is composed of interconnected molds that are more likely to be associated with selective dissolution of fossil

*This work was supported by the U.S. National Science Foundation through grant DMS-0074310.

fragments, or voids within or between fossils that were never filled with sediment [1].

We consider in this paper a vuggy medium; that is, a rock fabric with many (perhaps centimeter to decimeter scale) vugs scattered throughout its extent. Moreover, we are most interested in the case in which the vug system is interconnected. These types of multiscale rock fabrics are difficult to study mostly because they are on a scale that is too large to quantify using thin sections, and frequently on a scale that is too large to quantify adequately using core samples which are typically only a few centimeters in diameter. Nevertheless, our goal is to accurately predict the effective flow properties of these fabrics in aquifers on the field scale.

In work involving one of the authors, a macroscopic model for single phase, viscous fluid flow in a vuggy porous medium was derived by homogenization from the microscopic scale [2]. The macro-model yields to efficient computation, yet it apparently accounts for the micro-scale vug geometry so that it is able to predict the average flow behavior. We present in this paper some computational studies to support this hypothesis. We also show some computational results relating to the nature of the effective permeability of vuggy systems.

2. A MICRO-MODEL OF THE FLOW

In this section we recall a model governing a vuggy medium on a very fine scale. This model is theoretically and experimentally sound, but too detailed for field-scale applications. Darcy's law governs fluid flow in a porous medium on scales above the pore diameter [3–6]. Since the flow is expected to have a relatively low Reynolds number, the Stokes equations adequately models fluid flow in the vugs. Between the two flow regimes, the Beavers-Joseph-Saffman boundary condition holds [7–9]. This condition accounts for the fact that there is a nonzero tangential velocity to a free fluid at an interface with a porous solid.

Let the system domain be denoted by Ω. Then Ω consists of two parts, the vugs Ω_s and the porous matrix Ω_d, with an interface Γ between them. Let D be the symmetric gradient, i.e., $D\mathbf{v}$ is the matrix $\frac{1}{2}\left(\frac{\partial \mathbf{v}_i}{\partial x_j} + \frac{\partial \mathbf{v}_j}{\partial x_i}\right)$. The fluid velocity and pressure in the Stokes and Darcy regions are denoted $\mathbf{u}_s$, p_s and $\mathbf{u}_d$, p_d, respectively. These satisfy the following equations in the domain Ω (wherein μ is the fluid viscosity, g models gravity, f is an external source or sink, K is the matrix rock permeability, α is the Beavers-Joseph slip coefficient, ν_s is the unit normal pointing out of the Stokes domain Ω_s, and τ_i are unit tangent vectors to Γ):

Vugular region Ω_s (Stokes)

$$-2\mu\nabla\cdot D\mathbf{u}_s + \nabla p_s = g \quad \text{in } \Omega_s\ , \tag{1}$$

$$\nabla\cdot\mathbf{u}_s = f \quad \text{in } \Omega_s\ , \tag{2}$$

Rock matrix Ω_d (Darcy)

$$\mu K^{-1}\mathbf{u}_d + \nabla p_d = g \quad \text{in } \Omega_d\ , \tag{3}$$

$$\nabla\cdot\mathbf{u}_d = f \quad \text{in } \Omega_d\ , \tag{4}$$

Interface Γ

$$\mathbf{u}_s \cdot \nu_s = \mathbf{u}_d \cdot \nu_s \qquad \text{on } \Gamma \ , \tag{5}$$

$$2\nu_s \cdot D\mathbf{u}_s \cdot \tau_i = -\frac{\alpha}{\sqrt{K}}\mathbf{u}_s \cdot \tau_i \quad \text{on } \Gamma \ , \tag{6}$$

$$2\mu\nu_s \cdot D\mathbf{u}_s \cdot \nu_s = p_s - p_d \qquad \text{on } \Gamma \ . \tag{7}$$

The interface conditions represent continuity of mass flux (5), the Beavers-Joseph-Saffman condition on the tangential stress (6), and the continuity of normal stress (7).

3. A MACRO-MODEL AND THE EFFECTIVE PERMEABILITY

A macro-model of fluid flow in a vuggy medium has recently been derived from the micro-model through the mathematical theory of homogenization [2]. Briefly, one assumes that the geometric vug and pore structure of Ω is periodic of period Y, where Y is a reference cell, normally a rectangle in 2-D and a "brick" in 3-D. The reference cell is part vug Y_s and part matrix Y_d, with an interface γ between these regions.

Thus, Ω is a tessellation. For $0 < \epsilon \leq 1$, we create Ω^ϵ by tessellating the scaled cells ϵY. The homogenization problem is then to determine the behavior of fluid flow in Ω^ϵ as $\epsilon \to 0$, that is, as the fine scale becomes negligible. We must also scale both viscosity μ and permeability K by ϵ^2, since as $\epsilon \to 0$, flow paths (in our case vugs) become constricted, and a corresponding decrease in viscosity is required to maintain flow rates [5].

In the limit as ϵ vanishes, the fluid velocity $\mathbf{u}$ and pressure p converge (weakly) to a macroscopic velocity $\bar{\mathbf{u}}$ and pressure $\bar{p}$. What is important is that $\bar{\mathbf{u}}$ and $\bar{p}$ can be found by solving the macro-model

$$\mu\tilde{K}^{-1}\bar{\mathbf{u}} + \nabla\bar{p} = f \quad \text{in } \Omega \ , \tag{8}$$

$$\nabla \cdot \bar{\mathbf{u}} = q \qquad \text{in } \Omega \ . \tag{9}$$

That is, $\bar{\mathbf{u}}$ and $\bar{p}$ satisfy a Darcy equation on all of Ω, with an *effective permeability* matrix $\tilde{K}$ independent of the fluid viscosity. Moreover, the tensor $\tilde{K}$ is symmetric and positive definite, and it can be computed from the solution of a Darcy-Stokes problem posed on Y involving K, α, and the vug geometry.

To find the effective permeability $\tilde{K}$, one solves the following homogenized cell problem for each $\mathbf{e}_j$, the standard Cartesian unit vector in the jth direction, using periodic boundary conditions on ∂Y. It is a Darcy-Stokes system, and gives a periodic flux ω_j (and a periodic pressure ϕ_j, which we may discard):

$$-2\nabla \cdot D\omega_{j,s} + \nabla\phi_{j,s} = \mathbf{e}_j \quad \text{in } Y_s \ , \tag{10}$$

$$\nabla \cdot \omega_{j,s} = 0 \qquad \text{in } Y_s \ , \tag{11}$$

$$K^{-1}\omega_{j,d} + \nabla\phi_{j,d} = \mathbf{e}_j \qquad \text{in } Y_d \ , \tag{12}$$

$$\nabla \cdot \omega_{j,d} = 0 \qquad \text{in } Y_d \ , \tag{13}$$

$$\omega_{j,s} \cdot \nu_s = \omega_{j,d} \cdot \nu_s \qquad \text{on } \gamma \ , \tag{14}$$

$$2\nu_s \cdot D\omega_{j,s} \cdot \tau_i = -\frac{\alpha}{\sqrt{K}} \omega_{j,s} \cdot \tau_i \quad \text{on } \gamma \ , \tag{15}$$

$$2\nu_s \cdot D\omega_{j,s} \cdot \nu_s = \phi_{j,s} - \phi_{j,d} \qquad \text{on } \gamma \ . \tag{16}$$

We then compute the matrix $\tilde{K}$ from the formula

$$\tilde{K}_{i,j} = \frac{1}{V} \left\{ \int_{Y_s} \omega_{j,s,i} \, dv + \int_{Y_d} \omega_{j,d,i} \, dv \right\} , \tag{17}$$

where $\omega_{j,s,i}$ is the ith component of the vector $\omega_{j,s}$ and V is the volume (or area in 2-D) of Y.

4. A NUMERICAL METHOD

Both the micro-model (1)–(7) and the computation of the effective permeability (17) from (10)–(16) require the solution of a Darcy-Stokes system. Approximations of such systems in a non-vuggy context (i.e., in a medium with at most a few very large vugs) can be found in several papers (see, e.g., [10–12]). However, these computational methods treat the Darcy-Stokes interface in a special way. In our vuggy medium, the Darcy-Stokes interface is not isolated to a small portion of the domain, so the computational efficiency of these methods is compromised.

A new mixed finite element method using Stokes-type elements for second order elliptic equations (such as Darcy flow) was developed, and its convergence properties were analyzed in [13]. These elements are unlike the usual Raviart-Thomas elements [14] in that the Darcy velocity is approximated as a fully continuous vector function.

Since these finite elements apply to both Darcy and Stokes systems, it is natural to apply them to our vuggy medium [15]. The local basis functions are unchanged whether the element is Stokes or Darcy, and thus the sparsity structure of the global matrix is independent of the vug geometry. This makes it easy to write the code and develop an appropriate solver. In our computer code, we merely check to see if the element is Stokes or Darcy, and compute the local stiffness matrix appropriately. We also need to check to see if any part of the element boundary is on the Darcy-Stokes interface Γ, and add in the appropriate Beavers-Joseph-Saffman terms.

The only technicality is that the Beavers-Joseph-Saffman boundary condition implies that on the Darcy-Stokes interface there is a discontinuity in the tangential fluid velocity. Thus, in some configurations, when a Darcy element is next to a Stokes element, we need to relax the continuity of the finite elements. We can do this easily without compromising the matrix sparsity structure. Two of the current authors demonstrated and proved optimal computational convergence for the relaxed elements in [15], wherein a detailed description of these new elements can be found.

5. EXAMPLES OF EFFECTIVE PERMEABILITIES

In this section we consider the solution to the homogenized cell problem (10)–(16), and in particular the effective permeability that results from the formula (17). All our results are in 2-D.

The base case for our studies in this section is an 8 cm by 8 cm sample with Beavers-Joseph coefficient $\alpha = 1$, rock matrix permeability $K = 10$ md, and vugs with aperture $\delta = 1$ cm. We will consider varying these parameters and, especially, the vug configuration.

5.1. A layered medium

We begin with a study of a horizontally layered medium, which has a square reference cell $Y = (0, \ell) \times (0, \ell)$ with $Y_s = (0, \ell) \times (0, \delta)$ and $Y_d = (0, \ell) \times (\delta, \ell)$ (see Fig. 1), where $\ell = 8$ cm and usually $\delta = 1$ cm. In fact, this problem can be solved analytically [2]. The effective permeability that results is diagonal, and

$$\tilde{K}_{11} = \frac{1}{\ell}\left(\frac{1}{12}\delta^3 + \frac{\sqrt{K}}{2\alpha}\delta^2 + K(\ell - \delta)\right) , \tag{18}$$

$$\tilde{K}_{22} = \frac{\ell}{\ell - \delta}K . \tag{19}$$

Thus this subsection can be viewed more as a test that the code approximates the solution accurately.

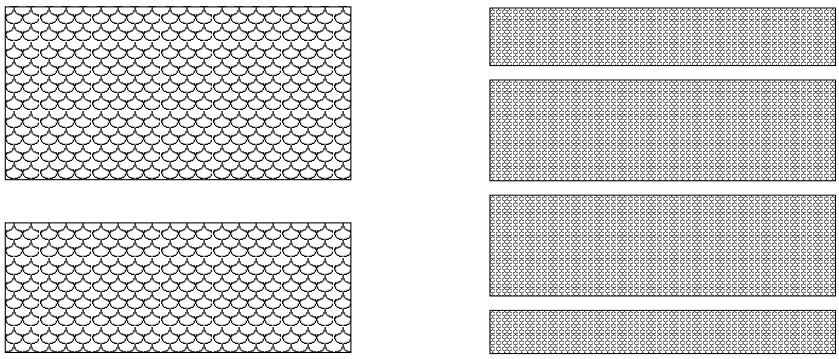

Figure 1. The layered medium. The reference cell is on the left, the periodic medium is on the right.

We begin with a convergence study on the base case. We show the results of varying the computational grid spacing h in Table 1. As can be seen, we obtain good convergence for even modest values of h. We generally take $h = 0.25$ cm henceforth.

Next we vary the Beavers-Joseph coefficient α. Results are tabulated in Table 2. We get excellent agreement with the analytical formula (18) for $\tilde{K}_{11}$, the x-permeability along the vug channel. Of course, the y-permeability is unaffected by the tangential slip due to α. Results of varying the rock matrix permeability K are given in Table 3, and again excellent agreement with the analytical formulas (18)–(19) results.

Perhaps a more interesting experiment is to vary the vug aperture δ. Results are shown in Table 4. Large aperture vugs result in effective x-permeabilities of a million to a billion times greater than that of the rock. However, even a tiny aperture of about 0.3 mm

Table 1
Numerical convergence for the layered medium.

h (cm)	$\tilde{K}_{11}$ (md)	$\tilde{K}_{22}$ (md)
1.00000	1.05550e+9	11.4286
0.50000	1.05549e+9	11.4327
0.25000	1.05549e+9	11.4332
0.12500	1.05548e+9	11.4334
0.00625	1.05548e+9	11.4335
0.03125	1.05548e+9	11.4335
0.00000	1.05548e+9	11.4286

The $h = 0$ results are the true analytical values from (18)–(19).

Table 2
Effect of varying the Beavers-Joseph coefficient α for the layered medium.

α	computed $\tilde{K}_{11}$ (md)	analytical $\tilde{K}_{11}$ (md)	computed $\tilde{K}_{22}$ (md)
0.01	1.06197e+9	1.06171e+9	11.4332
0.10	1.05610e+9	1.05605e+9	11.4332
1.00	1.05549e+9	1.05548e+9	11.4332
10.0	1.05543e+9	1.05543e+9	11.4332
100.	1.05542e+9	1.05542e+9	11.4332

Table 3
Effect of varying the rock matrix permeability K for the layered medium.

K (md)	computed $\tilde{K}_{11}$ (md)	analytical $\tilde{K}_{11}$ (md)	computed $\tilde{K}_{22}$ (md)	analytical $\tilde{K}_{22}$ (md)
1	1.05544e+9	1.05544e+9	1.1475	1.1429
10	1.05549e+9	1.05548e+9	11.433	11.429
100	1.05563e+9	1.05562e+9	114.29	114.29
1000	1.05610e+9	1.05605e+9	1142.9	1142.9

results in an x-permeability of some thousand times greater than K. Of course, the y-permeability is relatively unaffected by the presence of the vug, as the fluid is constrained to flow through the 10 md rock.

5.2. Flow through a meandering vug system

Except perhaps fractures, natural vugs are unlikely to maintain their orientation for long distances. We thus consider next the configuration depicted in Fig. 2, with a meandering

Table 4
Effect of varying the vug aperture δ for the layered medium.

δ (cm)	computed $\tilde{K}_{11}$ (md)	analytical $\tilde{K}_{11}$ (md)	computed $\tilde{K}_{22}$ (md)	analytical $\tilde{K}_{22}$ (md)
2.00000	8.44364e+9	8.44360e+9	13.3664	13.3333
1.00000	1.05549e+9	1.05548e+9	11.4327	11.4286
0.50000	1.31946e+8	1.31943e+8	10.6672	10.6667
0.25000	1.64955e+7	1.64949e+7	10.3227	10.3226
0.12500	2.06252e+6	2.06236e+6	10.1587	10.1587
0.06250	2.57967e+5	2.57926e+5	10.0787	10.0787
0.03125	3.22905e+4	3.22802e+4	10.0392	10.0392

vug channel of aperture $\delta = 1$ cm.

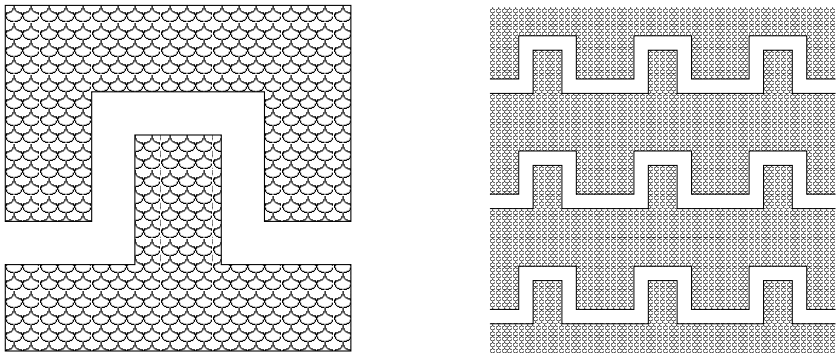

Figure 2. The meandering vug medium. The reference cell is on the left, the periodic medium is on the right.

In this case, the effective permeability is diagonal, with $\tilde{K}_{11} = 7.05195\text{e+}8$ md and $\tilde{K}_{22} = 17.8306$ md. Compare this to the layered case, for which $\tilde{K}_{11} = 1.05548\text{e+}9$ md and $\tilde{K}_{22} = 11.4286$ md. From the layered case, the meandering case has a decrease in x-permeability and an increase in y-permeability, as one should expect. Thus vug channel tortuosity has an important effect on the overall flow properties of the effective medium.

5.3. Flow through a constricted vug system

Natural vugs are unlikely to maintain their aperture, so we consider next a vug system which includes constrictions; it is illustrated in Fig. 3. The vug has aperture $\delta = 1$ cm, except the constriction, which is only 2 mm in aperture (and 2 cm in length). We obtain $\tilde{K}_{11} = 3.64777\text{+}7$ md and $\tilde{K}_{22} = 11.2495$ md. Comparing these to the system without a constriction ($\tilde{K}_{11} = 1.05548\text{e+}9$ md and $\tilde{K}_{22} = 11.4286$ md), we see that the y-permeability is essentially unchanged, but the x-permeability is reduced by a factor

of about 30. In fact, the x-permeability for a layered medium with a 2 mm channel is 8.44588e+6 md, which is only about 4 times smaller. We conclude that small constrictions have a significant effect on the overall flow.

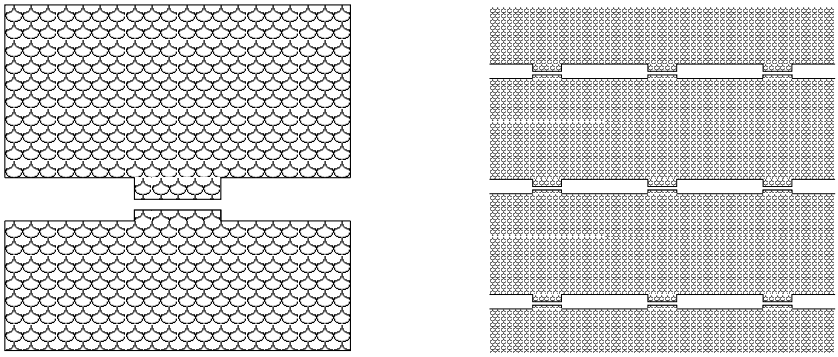

Figure 3. The constricted vug medium. The reference cell is on the left, the periodic medium is on the right.

5.4. Flow through a disconnected vug system

Finally, since some natural vuggy media are likely to have disconnected vugs, we study the effect of vug disconnectivity on overall effective permeability. We saw in the previous test that a medium with nearly disconnected vugs nevertheless results in a very large effective permeability. However, if the medium is disconnected, even by very small plugs between the vugs, we obtain permeabilities close to those for the matrix rock. We show this in a test on the configuration depicted in Fig. 4. In this configuration, the vugs are disconnected in the x-direction by a small plug of width that varies from 2 mm to 1 cm. Again, the vug aperture is 1 cm, so the plug is quite small. The computed effective permeabilities are given in Table 5. They are all within one order of magnitude of K. Thus, indeed, we have seen that vug connectivity or disconnectivity has a dramatic effect on effective flow properties.

Table 5
Effect of varying the plug between vugs for the disconnected medium.

plug (cm)	$\tilde{K}_{11}$ (md)	$\tilde{K}_{22}$ (md)
0.2	76.78	11.43
0.4	48.97	11.42
0.6	38.63	11.40
0.8	32.90	11.38
1.0	29.13	11.36

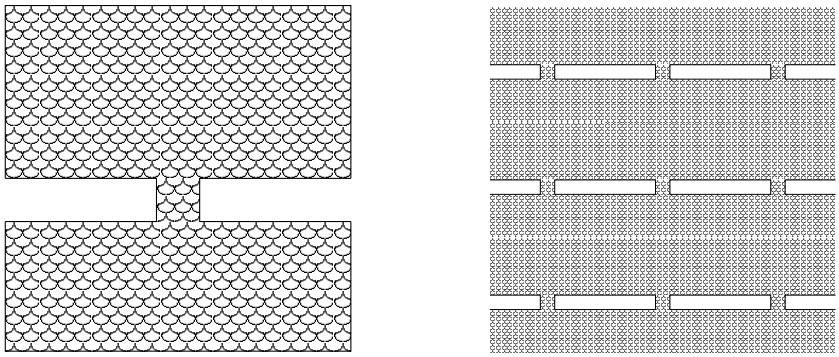

Figure 4. The disconnected vug medium. The reference cell is on the left, the periodic medium is on the right. The plug width (in the x-direction) varies from 2 mm to 1 cm.

6. A SIMPLE COMPUTATIONAL TEST OF THE MACRO-MODEL

In this section, we attempt to provide some verification of the accuracy of the macro-model in a simple test problem. This is necessary, since the homogenization process does not reflect reality in that ϵ does not tend to 0, we had to assume a particular ϵ scaling of μ and K, and, most importantly, natural vuggy media are not periodic. We may assume that the micro-scale model gives a physically relevant result, since the underlying equations are empirically and theoretically sound. We compute the macro-model prediction using $\tilde{K}$ in a Darcy flow simulator (actually the same code used to solve the Darcy-Stokes system), and then we compare these results to the fine-scale simulation.

6.1. Fine-scale results for pressure drop flow

We consider a small synthetic vuggy rock with an interconnected vug system, depicted in Fig. 5. The sample is 15 cm by 15 cm square, and we divide it into a fine scale grid of 30×30 cells (so the grid cells are 0.5 cm by 0.5 cm square). The vug channel is about 1 cm wide throughout its length. We set the matrix permeability $K = 10$ md and the Beavers-Joseph constant $\alpha = 1$.

We solve the Darcy-Stokes micro-model (1)–(7). We impose a unit pressure drop across the sample in the x-direction (i.e., $p = 1$ on the $x = 0$ cm boundary edge and $p = 0$ on $x = 15$ cm), and no flow boundary conditions on the other two boundary edges ($y = 0$ cm and $y = 15$ cm). We compute a net average fluid flux across the outflow edge, and multiply it by μ and the length of the sample 15 cm, to obtain an effective permeability $\tilde{k}_{\text{flux}} = 2.813\text{e+}8$ md of the sample in the x-direction.

6.2. Effective permeability of the sample

We next solve the reference cell problem (10)–(16) for the effective permeability (17). Using periodic boundary conditions, we obtain an effective x-permeability of only 52.31 md. This is 7 orders of magnitude too small. This result is easily understood, since when the sample is repeated periodically, it results in a system with disconnected vugs (see Fig. 5). Thus, the effective permeability is dominated by the matrix permeability.

To resolve this problem, we reflect the sample across the x-axis, creating a 30 cm

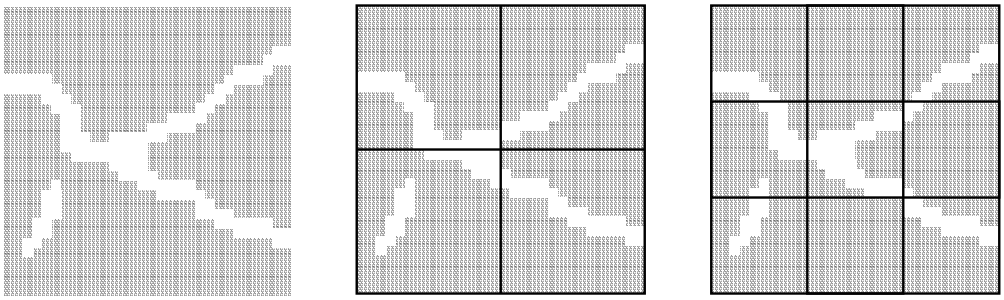

Figure 5. A synthetic vuggy rock with an interconnected vug system and an isolated vug. It is also divided into 2×2 and 3×3 coarse grids.

by 15 cm rectangular sample for which the vugs, when repeated periodically, remain interconnected. In this way, the periodic sample is governed by a geometrically and topologically similar vug system compared to the unreflected sample.

For the reflected sample, we obtained an effective x-permeability of $\tilde{K} = 2.813\text{e+}8$ md, the same as $\tilde{k}_{\text{flux}}$ from the pressure drop test. Thus average micro-scale flow computed from the periodic reference cell problem agrees with that from a more traditional pressure drop test computed also on the micro-scale.

6.3. Darcy computation using effective permeabilities

In practice, for full field-scale problems, we would need to solve the Darcy macro-model (8)–(9) on a coarse grid, using effective permeabilities (17) upscaling from the fine scale Darcy-Stokes cell problem (10)–(16). If we compute pressure drop flow across our small sample using only 1 grid cell, we will have the correct average flow, since $\tilde{K}$ and $\tilde{k}_{\text{flux}}$ agree. To illustrate both the importance of proper upscaling and using coarse grids, we next consider the problem on 2×2 and 3×3 coarse grids.

For a 2×2 coarse grid (see Fig. 5), we need to compute $\tilde{K}$ in each coarse cell, i.e., in each quarter of the original 15 cm by 15 cm domain. Extracting each quarter and reflecting the geometry in the x-direction as before, we obtain an effective x-permeability $\tilde{K}_{11}$ for each of the 4 coarse grid cells, which we show in a 2×2 array as

$$\tilde{K}_{11} = \begin{Bmatrix} 3.826\text{e+}8 & 1.605\text{e+}8 \\ 56.25 & 2.783\text{e+}8 \end{Bmatrix}.$$

Now solving the Darcy macro-model (8)–(9) leads to an effective flux permeability as before of $\tilde{k}_{\text{flux}} = 1.250\text{e+}8$ md, which is a bit low by a factor of about 2, but not a bad result, all things considered.

For a 3×3 coarse grid, reflecting the permeability as before, we obtain for each ninth of the sample an effective x-permeability

$$\tilde{K}_{11} = \begin{Bmatrix} 132.3 & 10.0 & 42.49 \\ 19.39 & 1.535\text{e+}9 & 10.98 \\ 12.97 & 10.0 & 5.114\text{e+}8 \end{Bmatrix}.$$

This is a disaster, since it is clear that the vug channel has disappeared! Only two coarse cells are dominated by the vugs, and the system as a whole is dominated by the matrix. That is, from Fig. 5 one can see that a 3×3 division results in coarse cells with vug channels that cross the coarse grid cell in the x-direction for only 2 cells (the two coarse cells with large $\tilde{K}$). The other cells appear to represent disconnected vug systems, even though the whole vug system is clearly connected. We obtain a flux x-permeability of only $\tilde{k}_{\text{flux}} = 21.19$ md.

To correct this problem, we use oversampling. That is, we compute the effective permeability of each coarse grid cell by solving the periodic Darcy-Stokes problem on the coarse grid cell and all of its nearest neighbors (and reflected in the x-direction). Thus, each corner cell sees the micro vug structure of 4 coarse cells, each cell adjacent to a boundary edge sees 6, and the center sees all 9. The oversampled effective permeability is

$$\tilde{K}_{11} = \begin{Bmatrix} 5.960\text{e+}8 & 1.900\text{e+}8 & 1.456\text{e+}8 \\ 3.973\text{e+}8 & 2.813\text{e+}8 & 2.637\text{e+}8 \\ 395.8 & 1235 & 2.577\text{e+}8 \end{Bmatrix}.$$

This permeability field retains the vug interconnectivity, and the flux x-permeability is $\tilde{k}_{\text{flux}} = 1.59919\text{e+}8$ (again low, but only by a factor of about 2).

7. CONCLUSIONS

This rather brief study allows us to make several important conclusions about modeling flow in vuggy media.

First, the effective permeability, as computed from (17) and (10)–(16), is mildly sensitive to vug channel shape, very sensitive to vug apertures, and extremely sensitive disconnectivities. That is, fluid flow in disconnected vug systems will be much like flow in the rock matrix; whereas, flow in connected vug systems are thousands to billions of times more permeable. Thus vug connectivity is the dominant consideration in understanding the flow.

Second, the simple test case of Section 6 supports the overall validity of the macromodel of Section 3. The computation of effective permeabilities using periodic boundary conditions is problematic in that periodic repetitions of the reference cell may artificially disconnect the vug channels. However, a reflection of the domain (we reflected in x, but in general one would need to reflect in both x and y—and z in 3-D) resolves this problem.

Third, upscaling vuggy media is complicated by the requirement that vug topology be maintained. If the vug system is rich enough within the coarse grid cell, as in the 2×2 coarse grid example, it will properly reflect global vug channels, and the effective permeabilities we compute appear to be be reasonable. However, if the vug system is cut up too finely by the coarse grid, as in the 3×3 coarse grid example, we may lose vug interconnectivity. For the example of this paper, we resolved this problem by oversampling.

REFERENCES

1. F. J. Lucia, Carbonate Reservoir Characterization, Springer-Verlag, New York, 1999.
2. T. Arbogast, H. L. Lehr, Homogenization of a Darcy-Stokes system modeling vuggy porous media, submitted.

3. J. Bear, Dynamics of Fluids in Porous Media, Dover, New York, 1972.
4. D. W. Peaceman, Fundamentals of numerical reservoir simulation, Elsevier, Amsterdam, 1977.
5. L. Tartar, Incompressible fluid flow in a porous medium—convergence of the homogenization process, in: E. Sanchez-Palencia, Non-homogeneous Media and Vibration Theory, Lecture Notes in Physics 127, Springer-Verlag, Berlin, 1980, pp. 368–377.
6. S. Whitaker, Flow in porous media I: A theoretical derivation of Darcy's law, Transport in Porous Media 1 (1986) 3–25.
7. G. S. Beavers, D. D. Joseph, Boundary conditions at a naturally permeable wall, J. Fluid Mech. 30 (1967) 197–207.
8. P. G. Saffman, On the boundary condition at the interface of a porous medium, Studies in Applied Mathematics 1 (1971) 93–101.
9. I. P. Jones, Low Reynolds number flow past a porous spherical shell, Proc. Camb. Phil. Soc. 73 (1973) 231–238.
10. A. G. Salinger, R. Aris, J. J. Derby, Finite element formulations for large-scale, coupled flows in adjacent porous and open fluid domains, International Journal for Numerical Methods in Fluids 18 (1994) 1185–1209.
11. D. K. Gartling, C. E. Hickox, R. C. Givler, Simulation of coupled viscous and porous flow problems, Comp. Fluid Dyn. 7 (1996) 23–48.
12. W. J. Layton, F. Schieweck, I. Yotov, Coupling fluid flow with porous media flow, SIAM. J. Numer. Anal. 40 (2003) 2195–2218.
13. T. Arbogast, M. F. Wheeler, A family of rectangular mixed elements with a continuous flux for second order elliptic problems, submitted.
14. R. A. Raviart, J. M. Thomas, A mixed finite element method for 2nd order elliptic problems, in: I. Galligani, E. Magenes (Eds.), Mathematical Aspects of Finite Element Methods, Lecture Notes in Math. 606, Springer-Verlag, New York, 1977, pp. 292–315.
15. T. Arbogast, D. S. Brunson, A computational method for approximating a Darcy-Stokes system governing a vuggy porous medium, submitted.